Wireless Personal Communications
https://doi.org/10.1007/s11277-026-12041-0

RESEARCH

Enhanced Channel Estimation for FBMC/OQAM Using M-IAM-LS-DNN Towards 6G

Nura A. Alhaj[1] · Mohd Faizal Jamlos[1,2] · Sulastri Abdul Manap[1] · Abdelmoneim A. Bakhit[1] · Mosab Hamdan[3] · Mohammed S. M. Gismalla[4]

Received: 5 August 2025 / Accepted: 14 April 2026

Abstract
Filter bank multicarrier/offset quadrature amplitude modulation (FBMC/OQAM) is a multicarrier modulation technique projected to replace orthogonal frequency division multiplexing (OFDM) in upcoming sixth-generation (6G) networks. However, because its orthogonality is confined to real-valued symbols, FBMC/OQAM suffers from intrinsic imaginary interference, which complicates channel estimation (CE) tasks. CE plays a crucial role in wireless communication systems; therefore, accurate CE is essential for next-generation networks, especially those supporting low-latency and vehicular applications. While evaluating channel characteristics accurately is critical, conventional CE methods are often inefficient. Recently, feedforward deep neural networks (DNNs) have garnered attention for their impressive performance in enhancing CE techniques. In this study, we propose and investigate a CE scheme based on neural networks, specifically the M-IAM-LS-DNN (Modified Interference Approximation Method Least Squares) approach, for FBMC/OQAM systems. This method uses neural networks to correct noise errors in LS channel estimation. According to simulation data, the suggested M-IAM-LS-DNN surpasses the conventional M-IAM-LS in terms of accuracy, by reducing the NMSE of the proposed M-IAM-LS-DNN for the 64 subcarriers scenario by 10% and the BER by 33% across a wide range of SNR levels.

Keywords Filter bank multicarrier · Offset quadrature amplitude modulation · Wireless communication · Channel estimation · Deep neural network algorithms · 6G

✉ Mohammed S. M. Gismalla
mohammed.gismalla@setu.ie

Mohd Faizal Jamlos
mohdfaizaljamlos@gmail.com

[1] Faculty of Electrical and Electronics Engineering Technology, Universiti Malaysia Pahang Al-Sultan Abdullah, 26600 Pekan, Malaysia

[2] Centre for Automotive Engineering Centre, Universiti Malaysia Pahang Al-Sultan Abdullah, Pekan 26600, Malaysia

[3] School of Computing, National College of Ireland, Dublin, Ireland

[4] Department of Engineering Technology, South East Technological University, Waterford, Ireland

Published online: 30 April 2026

1 Introduction

Unexpected growth in wireless communication has significantly impacted many aspects of our lives, creating diverse connectivity and capacity demands [1]. By the end of 2017 and the middle of 2018, the 3GPP (Third Generation Partnership Project) had finalized the standards for the SA (standalone) and NSA (non-standalone) versions of the 5G (Fifth Generation) Mobile Communication System [2]. However, due to the rapid expansion of wireless communication, there has been a growing need for the frequency spectrum and higher data rates [3]. In 2018, both the industry and researchers began to show interest in the concept of Sixth Generation (6G) communication [4, 5]. Wireless communications over 6G networks are expected to offer data rates of up to 1 Tbps, 1 ms latency, ultra-high connectivity, high reliability, and wide coverage, as well as support for fast mobility of up to 1000 km/h. To support new application such as smart cities, virtual and augmented reality, driverless cars, and other cutting-edge communication services [6, 7]. Multicarrier modulation, or MCM, is considered a promising approach to fulfill 6G criteria by dividing a wideband frequency-selective fading channel into multiple narrowband frequency-flat fading sub-channels. MCM improves robustness to channel impairments, reduces interference, and enables the transmission of massive amounts of data [8].

Lately, filter bank multicarrier-based/offset quadrature amplitude modulation (FBMC/OQAM), also referred to as OFDM/OQAM, has been proposed as a potential replacement for OFDM in 6G networks [9]. FBMC offers higher spectral efficiency than OFDM systems due to the absence of a cyclic prefix (CP) [10]. It also provides better resistance to the Doppler effect and carrier frequency offset (CFO) [11]. Accordingly, FBMC/OQAM is being explored in detail as a potentially useful solution for the next-generation physical layer. With well-designed prototype filters, FBMC/OQAM enables superior spectrum utilization in key future communication scenarios [1, 12, 13]. Each OQAM symbol comprises real and imaginary components, which are separated and transmitted as pairs of pulse-amplitude-modulated signals [14, 15]. However, only the real component of the symbols in FBMC/OQAM exhibits orthogonality [19, 20]. As a result, imaginary interference known as intrinsic imaginary interference arises between adjacent subcarriers transmitting real-valued symbols [15–17]. This interference contributes to increased bit error rate (BER) and mean-squared error (MSE) [18]. One approach to mitigating this issue is to introduce sufficient null guard symbols. However, spectral efficiency is lost with this strategy [19].

At the receiver, channel estimation (CE) is a continuous and essential operation that adapts to channel conditions to ensure accurate communication. CE is crucial for recovering data symbols and significantly impacts demodulation efficiency [20, 21]. Compared to OFDM systems, the CE process in FBMC systems is more complex [22]. The primary categories of CE in FBMC/OQAM are preamble-based and scatter-based approaches, both of which involve the addition of pilots [23]. A pilot or preamble is a known symbol that can be used (inserted) at the start of a frame and/or at random locations throughout the frame [24, 25]. This is a point of reference for calculating the transmitter-receiver channel response [28]. Preamble-based techniques are particularly important for time-invariant channels, aiming to achieve reliable and robust CE performance [26]. These techniques include the pairs of pilots (POP), the interference cancellation method (ICM), and the interference approximation method (IAM) [25–27].

Several IAM variations have recently been proposed to reduce intrinsic interference and enable the transmission of complex OQAM symbols to streamline receiver signal processing. Note that each IAM has a different preamble structure. Three FBMC/OQAM symbols with all zeros on the side, such as IAM-R (IAM-Real) and IAM-C (IAM-Complex). A modified IAM (M-IAM) is one of the IAM schemes; it improves CE performance while maintaining lower power consumption and larger magnitude than most other preamble designs [28]. Therefore, it will be used in this study.

Preamble-based least squares (LS) estimations are often unable to adequately capture unknown effects and noise defects commonly found in practical wireless communication networks. Ignoring noise during estimation is a major limitation of LS channel estimation. Although the minimum mean-square error (MMSE) CE is accurate, it requires knowledge of the channel and noise second-order statistics and is computationally intensive, making it less practical. Deep Learning (DL) has demonstrated exceptional capabilities in extracting complex patterns from raw data and holds promise for addressing CE challenges that conventional methods struggle with. In recent years, DL has been studied as a more effective alternative to traditional LS and MMSE-based CE techniques [29].

Feedforward deep neural networks have demonstrated success in various communication system applications, particularly in channel estimation (CE) techniques [30]. During training, a feedforward DNN in supervised learning transmits input features from one layer to the next. Multiple neurons provide weighted inputs to each neuron. Model performance is optimized by selecting hyperparameters after combining an internal activation function [29]. DNNs have addressed CE challenges in both FBMC and OFDM systems. One distinguishing characteristic of the deep channel estimator is that it requires only information obtained directly from the channel's received signal. DNNs eliminate the need to learn or understand channel statistics [31], making the estimator suitable for all channel types, including line-of-sight (LOS) and scattering channels.

Even though LSTM-based models are intended to represent temporal dependencies, when the channel coherence interval is short, as is typical in high-mobility 6G applications, they often introduce greater computational complexity, longer training periods, and convergence challenges. Similarly, when the Doppler spread is significant, CNNs that rely on local spatial feature extraction may not capture the nonlinear mapping between received pilot symbols and the underlying channel coefficients. CNN-LSTM hybrids can model both spatial and temporal correlations, but because they require many more parameters than our proposed DNN, they often overfit with constrained pilot resources. On the other hand, without relying on long-sequence memory methods, the proposed DNN is specifically designed to approximate the nonlinear channel estimation function. Faster convergence and improved generalization across SNR conditions and mobility patterns are enabled by its lightweight architecture. Compared with CNN, LSTM, Bi-LSTM, and CNN-LSTM architectures, the suggested model provides a more stable estimate and greater resilience, making it more appropriate for real-time 6G channel estimation [30].

Numerous studies, including those by Li et al. [34], have developed DNN-based approaches to overcome CE challenges. Who has used a DNN to increase performance; the outcomes are very complicated and rely on the pilots and the signal received. To sense and recover the downlink CSI in large MIMO systems, Wen et al. [32] developed a CsiNet DL-based system. When comparing the reconstruction quality of the recovered CSI with earlier compressive-sensing-based methods, CsiNet significantly improved it. A DL-based CE and

equalisation for FBMC systems was proposed by Cheng et al. [33]. They considered the CE, equalization, and QAM demapping as a "black box" in the DL-CE approach. In addition, the experimental results obtained under the pedestrian and vehicle A channel model showed that the proposed DL-CE scheme achieved a good estimation of BER.

A supervised DNN model based on a unique training technique was proposed by Bedoui et al. [34]. This approach required training using the relevant CIR and the pilot symbols that were received. To mitigate imaginary interference and enable MIMO technology with FBMC/OQAM, Bedoui et al. [35] proposed a DNN-based method. The simulations showed that the proposed approach increased the computational complexity significantly while maintaining good performance in terms of BER. Abusubaih et al. [36] developed a novel CE technique utilizing ResNet-deep neural networks. In the Res-DNN scheme, a Res-DNN model replaced the CE, equalization, and demapping modules. Simulation results show that the Res-DNN system outperforms other schemes based on BER. A ResNet-DNN neural network was also used by Wang et al. [37] to combine FBMC/OQAM with a DL model. Table 1 presents a detailed comparison of previous studies and the current work, highlighting the specific problems addressed, the proposed solutions, and the advantages and limitations of each approach.

A detailed simulation system was constructed, and the features and label processing of the incoming data were planned. Based on pilot estimation and simulation findings, the recommended approach outperforms OFDM and FBMC systems in terms of BER, noise resistance, and resilience. However, DNN research on CE in FBMC/OQAM is limited. In this work, we aim to offer an alternative method by implementing M-IAM-LS_DNN. This DL-based channel estimation strategy improves performance by using neural networks to correct LS channel estimation noise. This contrasts with previous research, which substitutes computationally demanding DL networks for the M-IAM-LS channel estimation. The contribution of this paper is:

- A detailed exploration of FBMC/OQAM, channel estimation, and feedforward deep neural networks (DNN).
- Enhancement of M-IAM-LS channel estimation performance using a fully connected feedforward DNN.
- A comparative analysis of the traditional LS method and the proposed M-IAM-LS-DNN in terms of BER and NMSE.
- A comprehensive evaluation of the impact of training SNR values on the performance of LS-DNN-based CE.

This paper aims to cover the following: the fundamental classical preamble-based (M-IAM-LS) channel estimation model for FBMC/OQAM waveforms is presented in Sect. 2. Proposed DNN-based CE schemes, neural network algorithms, backpropagation, and activation functions are defined and explained in Sect. 3. Simulation results are given in Sect. 4. Lastly, the conclusion of the paper is presented in Sect. 5.

Table 1 p rovides a comprehensive comparison of this study's achievements with previous research on channel estimation techniques

References	Problem	Methods	Block-based or model-driven	Result	Metric	Demerit
[27]	Enhance CE performance	Bayesian compressive sensing (BCS) channel and iterative fast Bayesian matching pursuit algorithm		According to the simulation results, the suggested approach outperforms traditional compressive sensing techniques in terms of MSE and BER.	BER and MSE	The suggested method's computing complexity has increased.
[38]	Enhance LS	LS-DFT (discrete Fourier transform)	–	It is better than conventional LS.	BER and MSE	Computational complexity due to using DFT.
[39]	Suppressing the intrinsic imaginary interference (IMI)	Time-domain least squares (TDLS)	–	Improves the optical channel estimation performance	BER and MSE	Computational complexity of matrix multiplication and inversion
[40]	Enhance channel estimation and minimize IMI.	KalCod (Kalman filter and CAP)	–	The updated KAP outperforms the others in terms of spectrum efficiency and estimation accuracy. It is also simple to implement.	BER, number of multiplications, and throughput.	The use and enhancement of the suggested methods using MIMO-FBMC/OQAM are not considered.
[41]	Enhance LS-CE and minimize IMI	Recursive weighted LS (RWLS)	–	Enhance the performance of equalization and channel estimation while achieving high transmission efficiency.	BER	The model is sensitive to the Doppler effect
[42]	Enhance CE performance	Polar codes	–	Polar codes exhibit comparable error-correcting capabilities.	BER	In FBMC-OQAM systems, polar codes are not appropriate for larger frame sizes.

Table 1 (continued)

References	Problem	Methods	Block-based or model-driven	Result	Metric	Demerit
[33]		Deep Neural Network (DNN)-based channel estimate	Block-based	Better in terms of BER and MSE than the LS algorithm, but worse than the MMSE method	BER and MSE	Highly complex.
[35]	Enhance channel estimation and minimize IMI.	DNN-based for MIMO	Block-based	Good performance in terms of BER		Highly complex.
[43]	Enhance LS	ANN LS-CEA	Model-driven Enhance the LS	It can reduce the BER performance by 50%.	BER	It cannot be ensured when the training periods are short. Additionally, it did not account for the channel's effect.
[33]	Enhance CE and minimize IMI	DNN	Block-based	DNN estimator performs better than conventional least squares (LS) estimator	BER and MSE	The mathematical model of the channel is not perfect.
[44]	Enhance CE performance	Deep bidirectional gated-recurrent unit (BiGRU) scheme.	Model-driven	Greatly enhances the CE performance	BER and MSE	The algorithm is highly complex and vulnerable to interference from both the front and rear symbols.
[45]	Enhance channel estimation and minimize IMI.	Res-DNN	Block-based	Significantly improve the performance of the downlink	BER and MSE	Computational complexity and memory requirements are high
This study	Enhance CE	M-IAM-LS-DNN	Model-driven	significantly improves the CE	BER and NMSE	More accurate by 33.3%for BER and 10% for NMSR, besides less complexity

2 System Model for M-IAM-LS Channel Estimation for FBMC/OQAM

The FBMC system, also known as OFDM/OQAM and staggered multi-tone (SMT), was proposed by Saltzberg and Chang in 1971, originating from the same family of OFDM techniques [46]. The FBMC/OQAM system comprises a synthesis filter bank (SFB) with parallel transmit filters at the transmitter and an analysis filter bank (AFB) at the receiver [47]. OQAM transmits real and imaginary samples with a shift of half the symbol time [41, 48]. In the synthesis filter bank (SFB) FBMC module, the inverse fast Fourier transform (IFFT) and polyphase filters make up the two core blocks [49]. The AFB filter module relies on two fundamental building blocks: the polyphase filter and the fast Fourier transform (FFT) [50], as illustrated in Fig. 1.

According to the Nyquist theory, the FBMC prototype filter was designed to achieve ideal time-frequency localization [1]. To achieve optimal frequency and temporal localization, a PHYDYAS Filter (PF) is implemented. The FBMC/OQAM technique is employed to improve the performance of wireless networks. The major drawback of FBMC/OQAM is the presence of imaginary interference, which makes channel estimation challenging [51]. The SFB discrete-time baseband transmitting a signal with even M subcarriers can be expressed as in [28].

$$\mathrm{s}\,(\mathrm{l}) = \sum_{\mathrm{m}=0}^{\mathrm{M}-1} \sum_{\mathrm{n}\in\,\mathrm{z}} \mathrm{d}_{\mathrm{m,n}} \mathrm{g}_{\mathrm{mn}} \tag{1}$$

$$\mathrm{g}_{\mathrm{mn}}\,(\mathrm{l}) = \mathrm{g}\left(\mathrm{l}-\mathrm{n}\frac{\mathrm{M}}{2}\right) \mathrm{e}^{\mathrm{j}\frac{2\pi m\ \left(l-\frac{\mathrm{lg}-1}{2}\right)}{\mathrm{M}}} \mathrm{e}^{\mathrm{j}\varnothing \mathrm{mn}} \tag{2}$$

$$\mathrm{s}\,(\mathrm{l}) = \sum_{\mathrm{m}=0}^{\mathrm{M}-1} \sum_{\mathrm{n}\in\,\mathrm{z}} \mathrm{d}_{\mathrm{m,n}}\, \mathrm{g}(\mathrm{l}-\mathrm{n}\frac{\mathrm{M}}{2})\, \mathrm{e}^{\mathrm{j}\frac{2\pi m(l-\frac{\mathrm{lg}-1}{2})}{\mathrm{M}}} \mathrm{e}^{\mathrm{j}\varnothing_{\mathrm{m,n}}} \tag{3}$$

.

where, $\mathrm{d}_{\mathrm{m,n}}$ is the real OQAM symbol, m,n are frequency time points, m is the subscriber index of the OQAM symbol, n is the time index, $\mathrm{g}(\mathrm{l}-\mathrm{n}\frac{\mathrm{M}}{2})$ is a true symmetric prototype filter's impulse response, $\mathrm{j}=\sqrt{-1}$ is the imaginary unit, M is the even number of subscribers, lg is the length of the filter $(lg = K \times M)K$ is the overlap factor and $\varnothing_{(\mathrm{m,n})}=(\mathrm{m}+\mathrm{n})\,\frac{\pi}{2}+\mathrm{mn}\pi$. Since the pulse g is constructed, the surrounding subcarrier functions $\mathrm{g}_{\mathrm{mn}}\,(\mathrm{l})$ are only orthogonal. This results in some ISI at the AFB output being completely imaginary. The imaginary interference width is given by [28]:

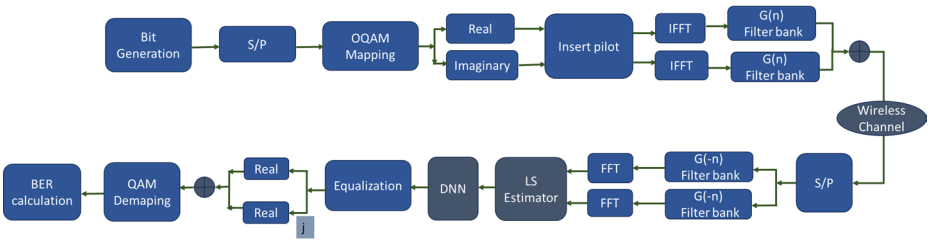

Fig. 1 Structure blocks of synthesis filter bank (SFB) and analysis filter bank (AFB)

$$\sum g_{mn}(l)\ g^{*}_{p,q}(l) = j < g >^{p,q}_{m,n} \tag{4}$$

where $< g>^{(p,q)}_{(m,n)}$ is the interference width in frequency-time (FT) between (p, q) and (m, n) FT points, "q" is the time index, and "p" is the subcarrier index of the OQAM symbol. Assuming the linear phase (coherence bandwidth), time-invariant (coherence time), and about equal power for each spectral component as they pass through the prototype filter. The AFB's output at the q^{th} FBMC symbol and p^{th} subcarrier is provided by [25, 28, 51]:

$$y_{(p,q)} = H_{(p,q)}\, d_{(p,q)} + I_{(p,q)} + \eta_{(p,q)} \tag{5}$$

where $I_{(p,q)} = j \sum_{m=0}^{M-1} \sum_{n} H_{(m,n)} d_{(m,n)} < g >^{(p,q)}_{(m,n)}$ is the imaginary interference, H_((p, q)) is the CFR (channel frequency response), and $\eta_{(p,q)}$ is a Gaussian noise component with zero mean and variance σ2. Assuming a precisely timed and localized pulse, a common assumption is that $I_{(p,q)}$ originated from the neighborhood of (p, q), first order, denoted as$\Omega_{(p,q)}$ equals (p, q±1)/(p±1, q ± 1)/(p ± 1, q). Equation (5) can be rewritten as follows if the CFR is approximately constant over this neighborhood:

$$y_{(p,q)} = H_{(p,q)}\, c_{(p,q)} + \eta_{(p,q)} \tag{6}$$

where $c_{(p,q)} = d_{(p,q)} + j u_{(p,q)}$ is the virtual signal of the transmitted signal symbol at (p, q) and given as:

$$u_{(p,q)} = \sum_{(m,n)\in\Omega_{p,q}} d_{(m,n)} < g >^{(p,q)}_{(m,n)} \tag{7}$$

The actual CFR ($\hat{H}_{(p,q)}$) can be obtained by the following equations at the corresponding FT point:

$$\hat{H}_{p,q} = \frac{y_{p,q}}{c_{p,q}} \tag{8}$$

$$\hat{H}_{p,q} = \frac{H_{p,q} c_{p,q} + \eta_{p,q}}{c_{p,q}} \tag{9}$$

$$\hat{H}_{p,q} = H_{p,q} + \frac{\eta_{p,q}}{c_{p,q}} \tag{10}$$

$$\hat{H}_{p,q} = H_{p,q} + \frac{\eta_{p,q}}{d_{p,q} + j u_{p,q}} \tag{11}$$

The objective is to find a preamble structure that maximizes the power of $\left(d_{(p,q)} + j u_{(p,q)}\right)$ while maintaining a low PAPR at the transmitter. Consequently, the accuracy of the estimation is enhanced as the power of $\left(d_{(p,q)} + j u_{(p,q)}\right)$ power [28, 52].

3 Feedforward Deep Neural Network (DNN)

Deep learning (DL) plays a crucial role in radio resource management, channel estimation, and mobility management [21, 53]. DL is used to map input features to predicted output values. It makes predictions and decisions based on the data it has learned [54, 55]. It can overcome the complexity of mathematical formulas and solve complex problems [36]. DL can be implemented in communication systems through both data-driven and model-driven methods [45]. The data-driven methodology views systems as black-box units, relying on pre-existing data and analysis, lacking specialized understanding, and requiring large datasets and varied network parameters for training. The model-driven approach, based on mathematical models, combines DL with traditional algorithms to enhance communication systems by replacing known blocks [56].

One of the DL algorithms, called DNN, aims to imitate the way information is transferred between biological neurons. It is composed of layers, each of which feeds into the one above it in a forward direction. The input layer represents the input, while the hidden layers lie between the input and output layers and contain neurons for parallel processing. The output layer is illustrated in Fig. 2; this figure also explains the structure of the DNN used in the study.

In supervised learning, a DNN repeatedly performs the process of sequentially passing input feature data from one layer's neurons to the neurons of the subsequent layer. Information is extracted at each stage and transferred to the subsequent layer; multiple other neurons provide weighted inputs to each neuron. After adding up all these inputs and passing them through an internal activation function, a hyperparameter is selected to optimize the model's performance. The Neural Network's weight can be adjusted throughout the training process based on feedback from prediction errors to enhance subsequent prediction improvements [57].

The data set used in this study was generated by using MATLAB code according to the ideal channel (without channel fading effect) and wih channel fading. It is computed using Eq. (11) and the parameters mentioned in Table 1. Batch training updates inputs once

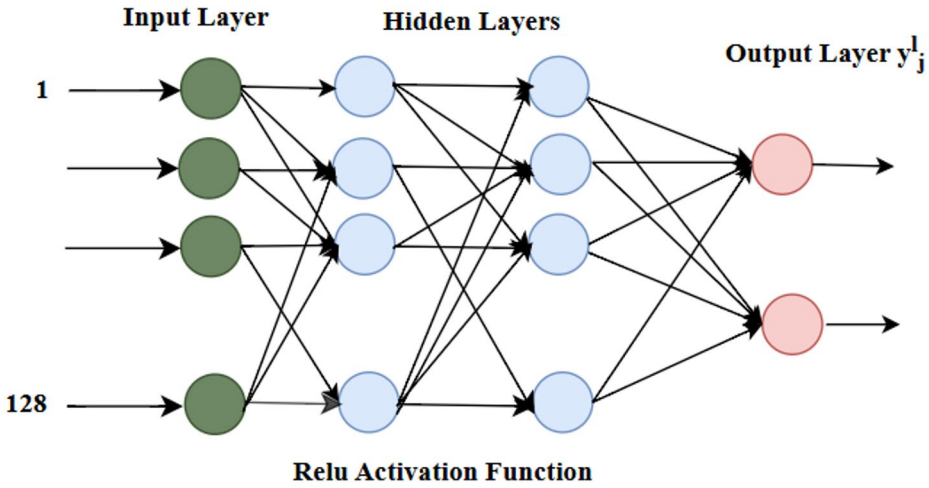

Fig. 2 Explain the structure of the DNN used in the study

they are entered into the NN, while incremental training updates weights instantly after each iteration, using backpropagation techniques to reduce errors [44]. NNs utilize non-linear activation functions, such as sigmoid, hyperbolic tangent, Gaussian error linear unit (GELU), rectified linear unit (ReLU), and SoftMax, to enhance learning capacity and model complex relationships.

$$y_j^l = f^{(l)} \sum_{i=0}^{N_l} \left(w_i^l y_{(i,j)}^{(l-1)}\right) + b_j^l \tag{12}$$

where N_l represents all neurons, b_j^l is the bias in j^{th} neuron, $w_{(i,j)}$ is the weight from i^{th} neuron in $(l\text{-}1)^{th}$ layer to the j^{th} neuron of l^{th} layer, and $f^{(l)}$ is the activation function of l^{th} layer [29]. The parameter $\theta = (W, B)$ denotes the weights and biases of the entire DNN and must be estimated during the learning process. It is common knowledge that a loss function called Loss (θ) calculated by the difference between the predicted y_j^P and the true y_j^T [58, 59]:

$$\text{Loss}\,(\theta) = \text{argmin}(y_j^P - y_j^T) \tag{13}$$

The suggested DNN aims to determine and adjust the LS channel estimation error by minimizing a cost function. Loss (θ) is the DNN when H is the ideal channel impulse response, and the input is the LS-estimated channel $\hat{H}_{LS}$. The input data (real and imaginary components) is normalized to have zero mean and unit variance to improve training, and weights are saved at the end of the training phase for the epochs with the highest training and validation accuracies. DNN employs the ADAM optimizer and mean squared error (MSE) as the loss function. All layers employ ReLU as the activation function; the output layer, however, does not use an activation function and therefore does not restrict the output value. The performance of the M-IAM-LS-DNN channel estimation. Systems are assessed in this section using normalized mean square error (NMSE) simulations and a bit error rate (BER).

The transmitter would generate the signal that will be transmitted via the channel, as described in Fig. 2. The channel is the medium through which electromagnetic waves propagate from a transmitter to a receiver. Unlike wired channels, wireless channels are susceptible to various impairments that can degrade signal quality, such as fading and the Doppler effect. This study focuses on the pedestrian A (Ped A), vehicle A (Veh A), vehicle B (Veh B) and roadside-to-vehicle (RTV) channel models. Table 2 describes the power profile and channel delay of the channel used in our simulations, including pedestrian A (Ped A), RTV (roadside-to-vehicle), and vehicle A (Veh A) environments.

This study uses MATLAB code to generate a dataset by adopting wireless models, including the Rayleigh and Rician fading channels. The implementation of the proposed scheme follows the process outlined in Fig. 2, based on the communication system details. The trained and tested datasets of M-IAM-LS-DNN were read from the saved datasets. The dataset was set to 10,000 samples to match the perfect channel frequency response (H_{f0}), as the label and the actual M-IAM-LS (H_{est}) frequency responses. This was done by splitting the dataset into 80:20 training and test ratios.

First, LS channel estimation was applied to the received preamble (M-IAM). As FBMC/OQAM separated the real and imaginary parts towards the resulting 2k, these were used as inputs for the DNN. The trained DNN uses the trained dataset and LS as inputs for

Table 2 The channel model [59]

Ped A											
Delay (ns)	0	110	190	410							
Average path gain (dB)	0	−9.7	−19.2	−22.8							
RTV											
Delay (ns)	0	1	2	100	101	102	200	201	300	301	400	401
Average path gain (dB)	0	0	0	−9.3	−9.3	−9.3	−20.3	−20.3	−21.3	−21.3	−28.8	−28.8
Veh A											
Delay (ns)	0	310	710	1000	1730	2510					
Average path gain (dB)	0	−1	−9	−10	−15	−20					

predicting CFR. At the end of the training, the corrected LS channel estimate $y^{L}_{\hat{\mathrm{H}}_{LS}}$ would be attained at the output layer. Input data were normalized to have a zero mean and unit variance, since differences in scale across input variables may increase the difficulty of training for the modeled problem. The proposed DNN uses mean squared error (MSE) as the loss function, with ADAM as the optimizer. Whereas the rectified linear unit (ReLU), $f_a(x) = \max(0,\ x)$ is used as the activation function for all but the output layer. The effect of ReLU does not saturate for positive values, introduces sparsity by setting all negative values to zero, and improves the learning process in deep networks. The proposed model was trained using the preprocessed dataset, a batch size of 32, and was trained for 500 epochs. The neural network model was constructed with 2 and 3 hidden layers (Fig. 3) to extract spatial features from the input data, followed by dense layers for decision-making. LS-DNN can be attributed to the DNN's ability to extract channel features and learn a meaningful representation of the given dataset. Two DNN architectures are suggested, each with a distinct number of hidden layers and nodes per hidden layer. Note from previous literature that an increased number of hidden layers would correspond to the system's computational complexity. Moreover, using a single hidden layer will not perform as well as a DNN architecture, as it lacks the deeper architecture and feature-extraction capabilities. Furthermore, using three or four introduces additional layers and parameters, thereby increasing the system's computational complexity.

4 Simulation Results

An accurate CE is essential for reliable data transmission and high spectral efficiency. This section presents simulation results for the M-IAM-LS-DNN and single-input single-output (SISO) system channel estimators in MATLAB. Random, Rayleigh fading, Rician fading channel models with Additive White Gaussian Noise (AWGN) were employed. The Rayleigh channel model is frequently used to describe the effects of multipath fading. A single FBMC/OQAM symbol has a total of "K = 64" sub-carriers with a sub-carrier spacing of "156:25 kHz". The metrics used for evaluating CE performance are NMSE and BER, plotted against signal-to-noise ratio (SNR). NMSE is calculated using the squared difference between channel frequency response "H" and the estimated channel "$\hat{H}$" given as the mean of " $\frac{(\mathrm{H}\text{-}\hat{\mathrm{H}})^2}{\mathrm{H}}$ ". BER is a metric quantifying the accuracy of CE in digital communication systems by measuring the rate of bit errors in received data compared to the total transmitted data bits. For the FBMC/OQAM model design, PHYDYAS filters with "$K = 4$", subcarriers of" $M = 64$ and $M = 512$" OQAM modulation, and the least square estimator were utilized. We employed two-channel models for the M-IAM-LS-DNN system, as shown in Table 3.

Figure 3 shows that the SNR used during training has a significant impact on DNN performance. The optimal prediction results are obtained from training at the maximum SNR value, which we define as 30 dB in this case. In reality, the DNN may learn the channel more effectively when trained at a high SNR value, as the channel's influence is greater in this SNR range than the impact of the noise. The amount of training samples also affects NMSE; therefore, a sufficiently large dataset is required. The ability of the DNN to extract channel characteristics and obtain an accurate representation of the input dataset. It is responsible for the enhanced performance of the LS-DNN. Figure 4a displays the equivalent BER results on

```
seed = 7
train_X, test_X, train_Y, test_Y = train_test_split( *arrays: XS, YS, test_size=0.2, random_state=seed)
print('Training samples: ', train_X.shape[0])
print('Testing samples: ', test_X.shape[0])

# Build the model.
init = TruncatedNormal(mean=0.0, stddev=0.05, seed=None)
model = Sequential([
    Dense(units=128, activation='relu', input_dim=128,
          kernel_initializer=init,
          bias_initializer=init),
    Dense(units=128, activation='relu',
          kernel_initializer=init,
          bias_initializer=init),
    Dense(units=128, kernel_initializer=init,
          bias_initializer=init)
])
```

Fig. 3 Explain the dense layers using PyCharm Software

Table 3 The parameter for the FBMC/OQAM-LS system

Parameter	Value
FFT/IFFT	512, 2048
Number of subcarriers (M)	512, 2048
Bit/symbols	2,4,6
Channel models	Rician fading and time-variant Rayleigh
Modulation	OQAM
Preamble	M-IAM
Prototype filter	K = 4
DNN	2& 3 Hidden layers
Number of epochs	500
Batch size	32

an end-to-end wireless transceiver. We consider an M-IAM-LS-DNN architecture trained over a range of 0 dB to 30 dB.

Additionally, Fig. 4(b) compares the NMSE of the M-IAM-LS-DNN and LS-DNN architectures across a broad range of SNR values for the RTV channel. Figure 4a and b demonstrate that the FBMC-LS channel estimation technique improved performance over the OFDM-LS approach, particularly in terms of BER and NMSE.

At all SNRs, the BER and NMSE of the M-IAM-LS-DNN significantly outperform those of LS. As SNR rises, the M-IAM-LS-DNN's performance improves. Therefore, training the proposed DNN at high SNR provides better generalization because the channel observations in this regime contain significantly less noise contamination, allowing the network to learn the intrinsic channel structure rather than fitting to noise. From an error-decomposition perspective, low-SNR training samples exhibit a significant stochastic error component, which increases the model's variance and causes the DNN to memorize noise patterns rather than the underlying channel response. In contrast, high-SNR data reduce this variance term and force the model to learn a cleaner and more physically meaningful mapping between the received pilots and the actual channel coefficients. This effect is consistent with the classical bias-variance trade-off; high-SNR training reduces variance without increasing bias, thereby improving robustness when the model is later tested across a wide range of SNR values.

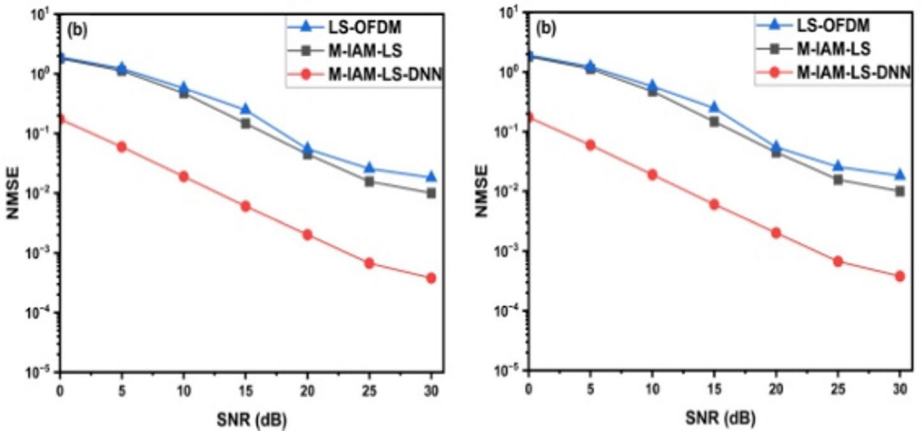

Fig. 4 (**a**) the BER and (**b**) NMSE performance for M-IAM-LS-DNN trained at various SNR levels using the RTV channel

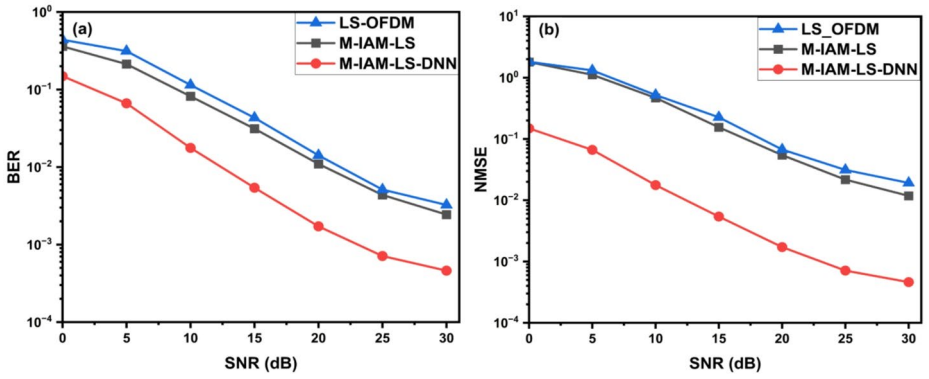

Fig. 5 Comparison of (**a**) the BER and (**b**) NMSE performance for M-IAM-LS-DNN using the Ped A channel

As SNR rises, the M-IAM-LS-DNN's performance improves. Comparable outcomes for BER and NMSE are also noted for Ped A, as shown in Fig. 5.

Furthermore, in practical wireless environments, the channel characteristics (e.g., multipath structure, delay profile, and Doppler dynamics) remain unchanged across SNR levels, while only the noise level varies. Therefore, training at high SNR enables the network to extract these stable, environment-driven features more effectively, resulting in superior BER and NMSE performance across all SNR ranges. Comparable outcomes for BER and NMSE are also noted for Ped A, as shown in Figs. 5a and b. As shown in the figure, SNR increases, and the BER decreases. However, the relatively high BER values indicate that LS may be suboptimal in this scenario. The BER values for LS-DNN are significantly lower than those for M-IAM-LS, especially at lower SNR levels. In this case, the proposed M-IAM-LS-DNN approach effectively improves channel estimation accuracy.

As demonstrated in Fig. 6a and b, with the Doppler effect equal to 1000 Hz and a vehicle speed of 200 km/h, the M-IAM-LS-DNN estimator performs well and outperforms the traditional LS estimator across all SNR levels in terms of both BER and NMSE in high mobility scenarios using the Vehicle A channel. However, this improvement is somewhat limited due to the channel characteristics.

Additionally, this study employs a time-invariant Rician fading channel model, chosen for its relevance in scenarios where a line-of-sight (LOS) component is present. Such channels are particularly significant in 6G applications, especially in microwave and satellite communications, where LOS propagation is dominant. Compared to Rayleigh fading, Rician fading provides superior BER performance at equivalent SNR levels, especially when the LOS component is strong. As illustrated in Fig. 7, both Rayleigh and Rician channels exhibit high BER at low SNRs; however, Rician consistently outperforms Rayleigh. In the moderate SNR range (5–15 dB), the BER for Rician fading drops more rapidly, while Rayleigh channels continue to experience severe fading. At higher SNRs, the BER under Rician fading becomes significantly lower, approaching the performance of an AWGN channel, due to the presence of a stable direct signal path. Furthermore, Fig. 7a demonstrates a substantial improvement in BER performance using the M-IAM-LS-DNN method, achieving a 12 dB gain over the traditional M-IAM-LS at a BER of 10^{-2}, along with a 15 dB improvement in NMSE as shown in Fig. 7b. These results confirm the effectiveness of the proposed DNN-assisted channel estimation method under Rician fading conditions.

Our proposed channel estimation method, based on a DNN, outperforms classical LS channel estimation schemes, as demonstrated clearly in Figs. 4 and 5, and 6. This indicates that the DNN can determine higher-order channel statistics. It specifically gains the ability to differentiate between channel gain and AWGN noise accurately.

In meeting the requirements of FBMC/OQAM systems, the Res-DNN method combines residual networks (ResNet) with deep neural networks (DNN). A ResNet (Residual Network) is a deep neural network that includes shortcut (skip) connections to solve the vanishing gradient problem in deep models. A Res-DNN deep learning model hereby replaces the traditional CE and equalization module, as well as the demapping module in the Res-DNN

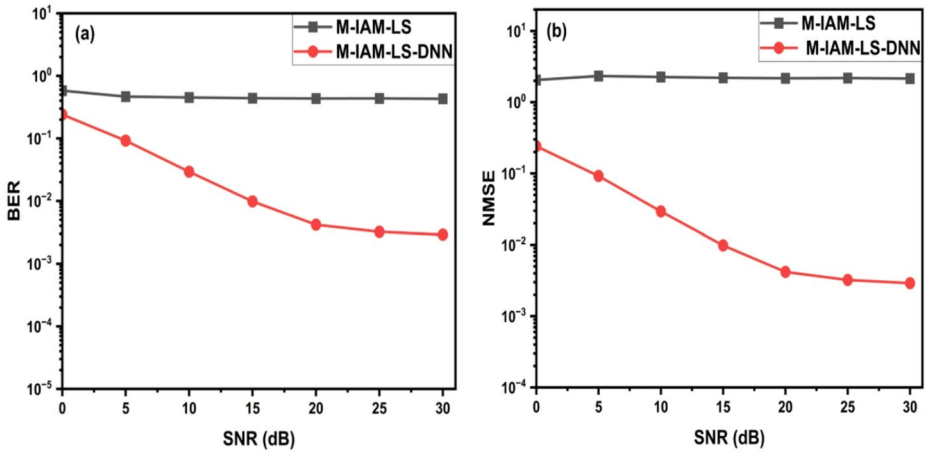

Fig. 6 Compare M-IAM-LS and M-IAM-LS-DNN in terms of (**a**) BER and (**b**) NMSE for v = 200 Km/h, fd = 1000 Hz when using the Vehicular A channel

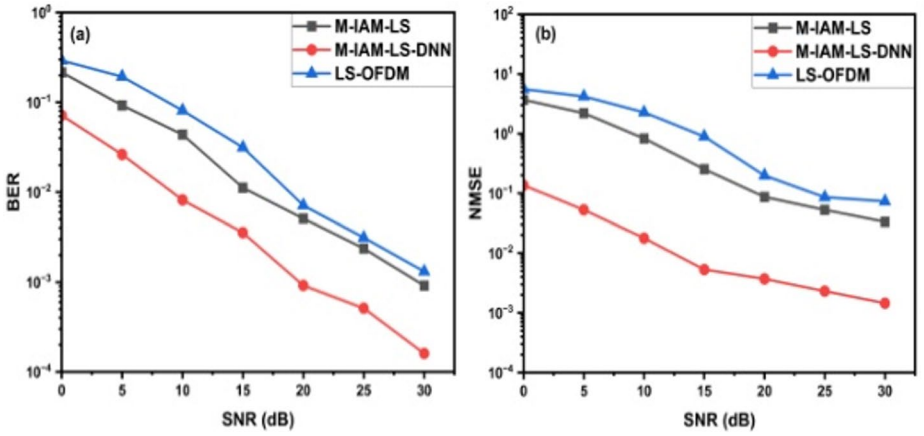

Fig. 7 (**a**) the BER and (**b**) the NMSE performance for M-IAM-LS-DNN using the RTV using the Rician channel

scheme. Res-DNN consists of 5 hidden layers in this model, including the input and output layers. My proposed DNN enhances existing DNN architectures by optimizing the network depth, activation functions, and training strategy to fit the characteristics of the communication channel better. Unlike ResNet, which focuses on intense residual mapping, my model maintains a moderate depth with adaptive normalization and dropout layers for stability and better generalization in FBMC channel estimation. Additionally, my DNN follows a model-driven learning approach, where the input is preprocessed using LS estimation before being refined by the neural network. This makes it more physically interpretable and more robust than pure ResNet-DNN structures.

A deep learning-based CE and equalization strategy would be employed in the deep learning (DL-CE) scheme. A DNN model learns the channel-state information and the constellation demapping technique in the DL-CE scheme. In other words, a DNN takes the position of the pilot extraction, channel equalization, and QAM demapping modules in the DL-CE model to constitute a total of an input layer, three hidden layers, and an output layer. As shown in Fig. 8, the suggested M-IAM-LS-DNN scheme has outperformed the DL-CE scheme in terms of BER, only being outperformed by the Res-DNN scheme in the Vehicular A channel, especially at higher SNR.

5 Conclusion

Although FBMC/OQAM is expected to be a crucial component of the future 6G wireless generation, its imaginary interference makes CE a complicated task. In order to enhance the M-IAM-LS channel estimator for FBMC/OQAM, correct noise error, and achieve accurate CE, this study proposes M-IAM-LS-DNN channel estimation algorithms based on deep learning. Initially, a survey was conducted, and the comparison between conventional CE approaches was presented. Subsequently, a discussion and evaluation of the suggested M-IAM-LS-DNN channel estimation technique is conducted for various SNR values. The recommended approach does not require prior knowledge of channel statistics. The pro-

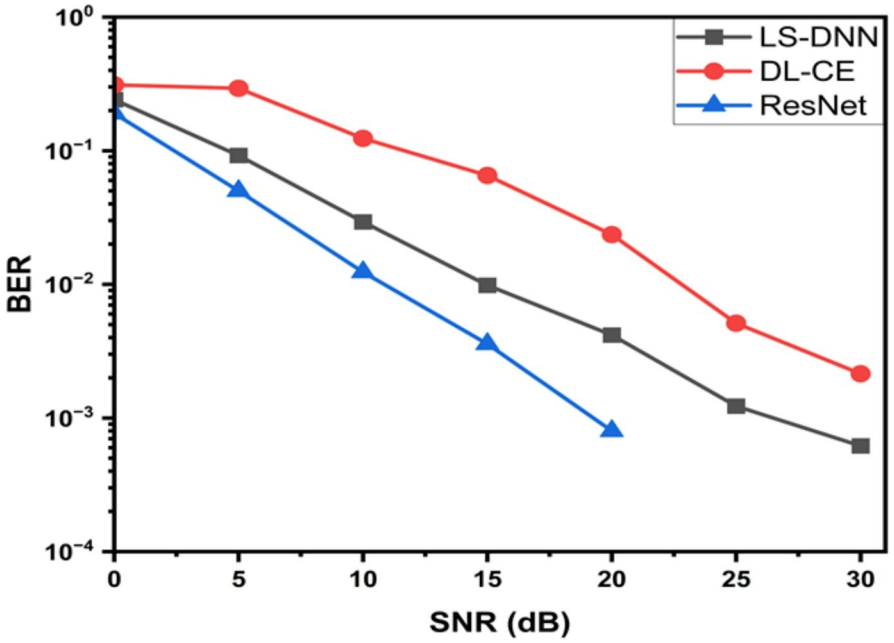

Fig. 8 The comparison of CE performance between our proposed M-IAM-LS-DNN, DL-CE, and ResNet schemes using a Vehicular A channel

posed M-IAM-LS-DNN technique significantly enhances channel estimation by reducing NMSE by 10% and BER by 33% over a wide range of SNR levels compared to the conventional M-IAM-LS method. Future studies need to focus on DL-based CE methods for high-mobility scenarios.

Author Contributions N.A Conceptualization, methodology, formal analysis, investigation, and original draft writing., M.J. Supervision, resources, investigation, writing—review and editing., S.A. Conceptualization, supervision, investigation, writing—review and editing., A.B. Validation, data curation, and software., M.H. Investigation, formal analysis, writing—review and editing., M.G. Methodology, formal analysis, writing—review and editing.

Funding Open Access funding provided by the IReL Consortium

Data Availability No datasets were generated or analysed during the current study.

Declarations

Competing interests The authors declare no competing interests.

References

1. Hamdar, F., Gussen, C. M. G., Nadal, J., Nour, C. A., & Baghdadi, A. (2023). FBMC/OQAM transceiver for future wireless communication systems: Inherent potentials, recent advances, research challenges. *IEEE Open Journal of Vehicular Technology, 4*, 652–666. https://doi.org/10.1109/ojvt.2023.3303034
2. Saad, W., Bennis, M., & Chen, M. (2019). A vision of 6G wireless systems: Applications, trends, technologies, and open research problems. *IEEE Network, 34*(3), 134–142.
3. Letaief, K. B., Chen, W., Shi, Y., Zhang, J., & Zhang, Y. J. A. (2019). The roadmap to 6G: AI empowered wireless networks. *IEEE Communications Magazine, 57*(8), 84–90. https://doi.org/10.1109/mcom.2019.1900271
4. Tariq, F., Khandaker, M. R. A., Wong, K. K., Imran, M. A., Bennis, M., & Debbah, M. (2020). A speculative study on 6G. *IEEE Wireless Communications*, *27*(4), 118–125.
5. Nikhila, Y., & Solomon, S. (2025). 6G wireless networking systems. *International Journal of AI and Machine Learning Innovations in Electronics and Communication Technology, 1*(1), 1–8.
6. Wang, H., Yan, T., Zhou, N., Li, X., Wen, F., & Du, W. (2025). Enhanced polar-domain channel estimation for near-field XL-MIMO in low-SNR scenarios. *IEEE Transactions on Vehicular Technology*.
7. Wang, H., Guo, P., Li, X., Wen, F., Wang, X., & Nallanathan, A. (2024). Mbpd: a robust algorithm for polar-domain channel estimation in near-field wideband xl-mimo systems. *IEEE Internet of Things Journal*.
8. Aldababseh, M., & Jamoos, A. (2014). Estimation of FBMC/OQAM fading channels using dual Kalman filters. *The Scientific World Journal*. https://doi.org/10.1155/2014/586403
9. E. Kofidis & D. Katselis. (2011). Improved interference approximation method for preamble-based channel estimation in FBMC/OQAM. In *2011 19th European signal processing conference (*pp. 1603–1607). IEEE.
10. Subalatha, M., Jayashri, S., & Raja, J. (2021). Low complexity maximum likelihood FBMC QAM for improved performance in longer delay channels. *Wireless Personal Communications, 117*(4), 3051–3066.
11. Kong, D., Zheng, X., Zhang, Y., & Jiang, T. (2020). Frame repetition: A solution to imaginary interference cancellation in FBMC/OQAM systems. *IEEE Transactions on Signal Processing*, *68*, 1259–1273.
12. Lv, S., Zhao, J., Yang, L., & Li, Q. (2020). Genetic algorithm based bilayer PTS scheme for peak-to-average power ratio reduction of FBMC/OQAM signal. *Ieee Access : Practical Innovations, Open Solutions*, *8*, 17945–17955.
13. Rebouh, D., Djebbar, A. B., & Besseghier, M. (2023). Blind joint CFO and STO estimation for FBMC/OQAM systems. *IEEE Communications Letters*. https://doi.org/10.1109/lcomm.2023.3293392
14. Čubrilović, Z., Kuzmanović, M., Punt, M., Vučić, D., & Kovačević, B. (2024). FBMC/OQAM-based secure voice communications over voice channels. *IEEE Access, 12*, 10565–10574.
15. Al-Rubaye, G. A. (2024). Comparison of MRC and SC techniques for OQAM/FBMC signals over combining NLD Rayleigh fading channel and IN for 5G. *AEU-International Journal of Electronics and Communications*, *184*, 155418–155418.
16. Gomes, R., Reis, J., Al-Daher, Z., Hammoudeh, A., & Caldeirinha, R. F. S. (2018). 5G: Performance and evaluation of FS-FBMC against OFDM for high data rate applications at 60 GHz. *IET Signal Processing, 12*(5), 620–628.
17. Cui, W., Qu, D., Jiang, T., & Farhang-Boroujeny, B. (2015). Coded auxiliary pilots for channel estimation in FBMC-OQAM systems. *IEEE Transactions on Vehicular Technology*, *65*(5), 2936–2946.
18. Singh, V. K., Flanagan, M. F., & Cardiff, B. (2019). Generalized least squares based channel estimation for FBMC-OQAM. *IEEE Access, 7*, 129411–129420.
19. Kofidis, E. (2021). On preamble-based FBMC/OQAM highly frequency selective channel estimation without guard symbols. In *2021 IEEE Global Communications Conference (GLOBECOM)* (pp. 1–6). IEEE.
20. Liang, S., Wang, C., Cao, H., Feng, J., & Sun, W. Channel estimation algorithm for IM/DD-OFDM/OQAM-PON system in industrial internet based on compressed sensing. In *2022 IEEE International Conference on Communications Workshops (ICC Workshops)* (pp. 1189–1194). IEEE.
21. Wang, H., Memon, F. H., Wang, X., Li, X., Zhao, N., & Dev, K. (2023). Machine learning-enabled MIMO-FBMC communication channel parameter estimation in IIoT: A distributed CS approach. *Digital Communications and Networks, 9*(2), 306–312.

22. Kofidis, E., Katselis, D., Rontogiannis, A., & Theodoridis, S. (2013). Preamble-based channel estimation in OFDM/OQAM systems: A review. *Signal Processing, 93*(7), 2038–2054.
23. Lu, X., Jiang, Y., Li, J., Yan, W., Tu, X., & Qu, F. (2023). Time-varying channel estimation and symbol detection for underwater acoustic FBMC-OQAM communications. *Journal of Marine Science and Application, 22*(3), 636–649.
24. Xue, L., Qiu, S., Wu, P., & Chen, D. (2019). An improved interference cancellation channel estimation method for OQAM/OFDM system. *Journal of Physics: Conference Series, 1169*(1), Article 12053.
25. El-Ganiny, M. Y., Khalaf, A. A. M., Hussein, A. I., & Hamed, H. F. A. (2021). A preamble based channel estimation methods for FBMC waveform: A comparative study. *Procedia Computer Science, 182*, 63–70.
26. Liu, W., Chen, D., Schwarz, S., Rupp, M., & Jiang, T. (2020). Preamble power optimization based on intrinsic interference utilization for OQAM/FBMC channel estimation. *IEEE Transactions on Vehicular Technology, 69*(11), 13556–13566. https://doi.org/10.1109/TVT.2020.3030661
27. Wang, H., Du, W., Wang, X., Yu, G., & Xu, L. (2020). Channel estimation performance analysis of FBMC/OQAM systems with Bayesian approach for 5G-enabled IoT applications. *Wireless Communications and Mobile Computing*. https://doi.org/10.1155/2020/2389673
28. Roshdy, R. A., Aboul-Dahab, M. A., & Fouad, M. M. (2020). A modified interference approximation scheme for improving preamble based channel estimation performance in FBMC system. *arXiv preprint arXiv.11676*
29. Gizzini, A. K., Shrey, S., Darak, S. J., Saurabh, S., & Chafii, M. (2022). Deep Neural Network Augmented Wireless Channel Estimation on System on Chip, *arXiv preprint arXiv:2209.02213*,.
30. Shen, G. X., Khandaker, M. R. A., & Tariq, F. (2020). Learning the wireless channel: A deep neural network approach. In *2020 International Conference on UK-China Emerging Technologies (UCET)*(pp. 1–6). IEEE.
31. Balevi, E., Doshi, A., & Andrews, J. G. (2020). Massive MIMO channel estimation with an untrained deep neural network. *IEEE Transactions on Wireless Communications*, *19*(3), 2079–2090.
32. Wen, C. K., Shih, W. T., & Jin, S. (2018). Deep learning for massive MIMO CSI feedback. *IEEE Wireless Communications Letters, 7*(5), 748–751.
33. Cheng, X., Liu, D., Wang, C., Yan, S., & Zhu, Z. (2019). Deep learning-based channel estimation and equalization scheme for FBMC/OQAM systems. *IEEE Wireless Communications Letters*, *8*(3), 881–884.
34. Bedoui, A., & Et-tolba, M. A neuro-fuzzy based detection approach for HARQ-CC in FBMC-OQAM systems. In *2020 9th IFIP international conference on performance evaluation and modeling in wireless networks (PEMWN)*(pp. 1–7). IEEE.
35. Bedoui, A., & Et-tolba, M. (2021). A Deep Neural Network-Based Interference Mitigation for MIMO-FBMC/OQAM Systems. *Frontiers in Communications and Networks*, *2*, 728982–728982.
36. Abusubaih, M. (2022). Intelligent wireless networks: Challenges and future research topics. *Journal of Network and Systems Management*. https://doi.org/10.1007/s10922-021-09625-5
37. Wang, Z., & Yuan, W. (2020). Channel estimation and detection method for multicarrier system based on deep learning. *Journal of ZheJiang University (Engineering Science)*, *54*(4), 732–738.
38. Alaghbari, K. A., Lim, H. S., & Eltaif, T. (2019). An improved least squares channel estimation algorithm for coherent optical FBMC/OQAM system. *Optics Communications, 439*, 141–147.
39. Fang, X., Xu, Y., Chen, Z., & Zhang, F. (2015). Time-domain least square channel estimation for polarization-division-multiplexed CO-OFDM/OQAM systems. *Journal of Lightwave Technology*, *34*(3), 891–900.
40. Elghetany, S. E., Hassaneen, S., Shaalan, I. E., & Soliman, H. Y. M. (2024). Channel estimation techniques based on intrinsic interference mitigation for FBMC/OQAM systems. *Computers and Electrical Engineering*, *117*, 109244–109244.
41. Ren, D., Li, J., Lu, G., & Ge, J. (2021). Joint channel estimation and equalization using new AFB output signal models for FBMC/OQAM systems. *IEEE Transactions on Communications*, *69*(6), 4186–4201.
42. Abose, T. A., Ayana, F. O., Olwal, T. O., & Marye, Y. W. (2024). BER performance analysis of polar-coded FBMC/OQAM in the presence of AWGN and Nakagami-m fading channel. *AIMS Electronics & Electrical Engineering*. https://doi.org/10.3934/electreng.2024014
43. Wang, X., Wang, X., & Cao, H. (2022). ANN LS-based channel estimation algorithm of IM/DD-OFDM/OQAM-PON systems with SDN Mobile Fronthaul Network in 5G. In *2022 IEEE International Conference on Communications Workshops (ICC Workshops)* (pp. 1195–1200). IEEE.
44. Raslan, W. A., Mohamed, M. A., & Abdel-Atty, H. M. (2022). Deep-BiGRU based channel estimation scheme for MIMO–FBMC systems. *Physical Communication, 51*, Article 101592–101592.
45. Cheng, X., Liu, D., Zhu, Z., Shi, W., & Li, Y. (2018). A ResNet-DNN based channel estimation and equalization scheme in FBMC/OQAM systems. In 2018 *10th International Conference on Wireless Communications and Signal* Processing *(WCSP)*(pp. 1–5). IEEE.

46. Patle, M. T. S. R., & Agrawal, M. D. (2021). Survey paper on performance evaluation of 5G system using filter bank multicarrier techniqueInternational journal of scientific research in science, engineering and technology. *International Journal of Scientific Research in Science, Engineering and Technology, 8*(3), 332–338.
47. Alhaj, N. A., Jamlos, M. F., Manap, S. A., Bakhit, A. A., & Mamat, R. (2022). A Review of Multiple Access Techniques and Frequencies Requirements towards 6G. In *2022 IEEE International RF and Microwave Conference (RFM)* (pp. 1–4). IEEE.
48. Bellanger, M. (2010). FBMC Physical Layer: A Primer, PHYDYAS FP7 Project Document.
49. Alhaj, N. A. (2023). Integration of Hybrid Networks, AI, Ultra Massive-MIMO, THz Frequency, and FBMC Modulation Towards 6G Requirements: A Review. *IEEE Access*.
50. Song, Z. Performance Evaluation of Prototype Filter-based FBMC/OQAM System for Wireless Communications, in 2024 *4th Asia-Pacific Conference on Communications Technology and Computer Science (ACCTCS)*, 2024: IEEE, pp. 776–779.
51. Alhaj, N. A. (2024). A Review on Preamble-Based Channel Estimation Method for FBMC/OQAM Toward 6G: Advantages, Challenges and Future Works. *Journal of Advanced Research in Applied Sciences and Engineering Technology*, pp. 63–80.
52. Lele, C., Siohan, P., & Legouable, R. (2008). 2 dB better than CP-OFDM with OFDM/OQAM for preamble-based channel estimation, in *2008 IEEE International Conference on Communications*, : IEEE, pp. 1302–1306.
53. Du, J., Jiang, C., Wang, J., Ren, Y., & Debbah, M. (2020). Machine learning for 6G wireless networks: Carrying forward enhanced bandwidth, massive access, and ultrareliable/low-latency service. *IEEE Vehicular Technology Magazine, 15*(4), 122–134. https://doi.org/10.1109/mvt.2020.3019650
54. Li, Y. (2017). Deep reinforcement learning: An overview, *arXiv preprint arXiv:1701.07274*,.
55. Zhang, S., & Zhu, D. (2020). Towards artificial intelligence enabled 6G: State of the art, challenges, and opportunities. *Computer Networks, 183*, 107556–107556. https://doi.org/10.1016/j.comnet.2020.107556
56. Lv, C., & Luo, Z. (2023). Deep learning for channel estimation in physical layer wireless communications: Fundamental, methods, and challenges. *Electronics, 12*(24), 4965–4965.
57. Cömert, Z., & Kocamaz, A. (2017). A study of artificial neural network training algorithms for classification of cardiotocography signals. *Bitlis Eren University journal of science and technology*, *7*(2), 93–103.
58. Gizzini, A. K., Chafii, M., Nimr, A., & Fettweis, G. (2020). Enhancing least square channel estimation using deep learning. In *2020 IEEE 91st Vehicular Technology Conference (VTC)* (pp. 1–5). IEEE.
59. Gizzini, A. K. (2021). *Advanced linear and deep learning based channel estimation techniques in doubly dispersive environments*. Cergy Paris CY Université.

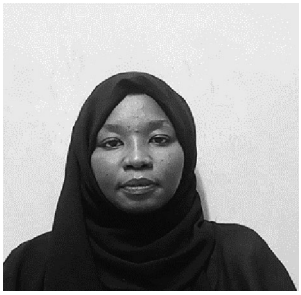

Nura Abdalrhman Alhaj received M.Sc. in 2017 from University of Sudan for Science and Technology, Khartoum, Sudan. Previously, she obtained his first degree from Faculty of Bayan, Sudan, with Honours, in Electronic Systems Engineering (Communication) in 2013. She is currently a Ph.D student in College of Engineering, Universiti Malaysia Pahang (UMP). Her research interests are Networking, Wireless Communication, and THz Communication.

Mohd Faizal Jamlos received Ph.D. in 2010 from Universiti Teknologi Malaysia, Johor, Malaysia and M.Sc. in 2008 from University of Adelaide, South Australia, Australia. Previously, he obtained his first degree from Universiti Malaysia Perlis, Malaysia, with Honours, in Computer Engineering in 2006. He is currently a full Professor in College of Engineering, Universiti Malaysia Pahang (UMP). He has co-authored some 250 scientific publications in peer-reviewed journals and conferences. His research interests are THz sensing, Internet-of-Things (IoT), Metamaterials, Data analytics, On-platform antennas and microwave circuitry. He is project leader of more than RM 3 Million in total funded by industries, government and university. He also active in providing consultations and trainings on Test Measurement system, Networking and IoT to various companies and universities. He is a practice professional Engineer of Board of Engineers Malaysia (BEM), Senior Member of IEEE, a National Medical Researcher (NMRR) and Corporate Member of Institute Engineers Malaysia (MIEM).

Sulastri Abdul Manap received her bachelor's degree of electrical engineering in 2003 from Universiti Teknologi Malaysia and earned her master's degree of Engineering in 2012 from University of Malaya. She is now a lecturer in Faculty of Electrical Engineering Technology, Universiti Malaysia Pahang. Her area of research is in wireless communication, specifically in radio resource management, and optimization.

Abdelmoneim Mohamedosman received a B.E. in Electronics and Communication from the Academy of engineering sciences, Sudan, in 2015, and currently, he is a master's student at Universiti Teknologi Malaysia Johor Bahru, Department of Electronic and Telecommunication. He is currently a research assistant and a PhD student at Universiti Malaysia Pahang (UMP). He was a teaching assistant from 2015 to 2018 at (the Academy of engineering sciences, AlMughtaribeen and Razi) Universities. His research interests include network routing algorithms, wireless sensor networks, antenna propagation, IoT, 5G communications, reliability of novel computer architectures such as embedded systems and machine learning.

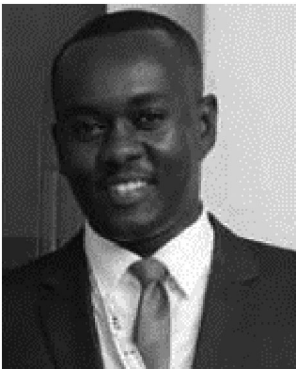

Mosab Hamdan (Senior Member, IEEE) received the B.Sc. degree in computer and elec tronic systems engineering from the University of Science and Technology (UST), Omdurman, Sudan, in 2010, the M. Sc. degree in computer architecture and networking from the Univer sity of Khartoum, Khartoum, Sudan, in 2014, and the Ph.D. degree in electrical engineering (computer networks) from Universiti Teknologi Malaysia (UTM), Johor Bahru, Malaysia, in 2021. From 2010 to 2015, he was a Teaching Assistant and a Lecturer with the Department of Computer and Electronic Systems Engineering, UST. He was a Research Fellow with several esteemed institutions, including UTM; Uni versiti Malaysia Sabah, Kota Kinabalu, Malaysia; the University of São Paulo, São Paulo, Brazil; the King Fahd University of Petroleum and Miner als, Dhahran, Saudi Arabia; and South East Technological University. He is currently an Assistant Professor with the School of Computing, National College of Ireland, Dublin, Ireland. His research interests include computer networks, network security, software-defined networking, the Internet of Things, intelligent transportation systems, and future networks.

Mohammed S. M. Gismalla received his B.Sc. (Hons) in Electronic and Electrical Engineering (Communications) from the International University of Africa (IUA), Sudan, in 2010, and his M.Sc. in Electronic Engineering (Communications) from Sudan University of Science and Technology in 2015. He completed his Ph.D. in Electrical Engineering (Communications) at Universiti Tun Hussein Onn Malaysia (UTHM) in March 2021. From 2010 to 2017, he worked as a Teaching Assistant and later as a Lecturer in the Department of Communication Engineering at IUA and the University of Bahri. He then joined the Lightwave Communication Research Group at Universiti Teknologi Malaysia (UTM) as a Postdoctoral Fellow, followed by a Postdoctoral Fellowship at the Center for Communication Systems and Sensing at King Fahd University of Petroleum and Minerals (KFUPM), Dhahran, Saudi Arabia. Dr. Gismalla later served as a Postdoctoral Researcher at the Walton Institute for Information and Communication Systems Science at South East Technological University (SETU), Ireland. He is currently an Assistant Lecturer in the Department of Engineering Technology at SETU and is a Senior Member of the IEEE. His research interests span quantum communication, visible light communication, free-space optical systems, optical and satellite communications, non-terrestrial networks including UAVs and HAPs, and emerging 5G/6G technologies.